Desalination and Water Treatment
www.deswater.com

doi: 10.5004/dwt.2020.25213

182 (2020) 288–298
April

Photocatalytic degradation of zidovudine by 0.8% ruthenium doped titanium dioxide nanoparticles during water treatment: synthesis, characterisation, kinetics and mechanism

Vijaykumar S. Bhamare*, Raviraj M. Kulkarni

Department of Chemistry, KLS Gogte Institute of Technology (Autonomous), Affiliated to Visvesvaraya Technological University, Belagavi - 590 008, Karnataka, India, Tel. +91 9449466448; email: vbhamare37@gmail.com

Received 29 January 2019; Accepted 24 November 2019

ABSTRACT

Photo-degradation of pharmaceutical drug zidovudine (ZDV) by synthesized ruthenium doped titanium dioxide nanoparticles (RDTDONPs) at 254 nm and pH (4.0 to 8.0) was investigated. 0.2%, 0.4%, 0.6%, and 0.8% (mole ratio) RDTDONPs were prepared by liquid impregnation method and characterised by different sophisticated techniques. Three photo-degraded products of ZDV are analysed. The photo-generated electron-hole pair mechanism was proposed in agreement with kinetic data. The calculated average crystallite size of 0.8% (mole ratio) RDTDONPs is 14.38 nm using the Scherrer equation. This smaller average crystallite size of 0.8% (mole ratio) RDTDONPs enhances the rate of mineralization due to the increase in surface area of nanoparticles. The effect of different parameters on the rate of mineralization of ZDV was investigated. The rate of mineralization of ZDV increases with the initial increase in [ZDV]. The rate of mineralization of ZDV was found higher in acidic conditions than alkaline conditions. Experimental results show that the rate of mineralization of ZDV moiety was found to be increased with an increase in the dosage of 0.8% (mole ratio) RDTDONPs. The rate of mineralization of ZDV was found to be increased with an increase in % doping of ruthenium from 0.2% to 0.8% (mole ratio) and then decreased beyond 0.8% ruthenium doping. The kinetic data reveals that the rate of mineralization of ZDV increases with an increase in light intensity.

Keywords: Water treatment; Emerging contaminants; Ruthenium doped titanium dioxide nanoparticles; Photocatalysis; Degradation; Characterisation; Zidovudine; Kinetics; Mechanism

1. Introduction

Pharmaceutical drugs have been consumed on a large scale by living beings to cure diseases and are detected in the aquatic environment by many advanced techniques. These emerging water contaminants have a detrimental effect on human beings, animals and aquatic organisms [1]. It is very much essential to remove emerging contaminants from an aquatic environment to make it safe and secure for our next generations [2]. Many conventional and biological techniques were reported in the earlier studies and not found capable to eliminate emerging water contaminants [3]. Therefore, there was a necessity of new advanced methods to eliminate the toxic organic contaminants detected in the aquatic environment. A literature study reveals that advanced oxidation processes (AOPs) are found to be capable of the complete mineralization of emerging water contaminants into harmless products [4]. AOPs generate highly powerful hydroxyl radicals that degrade the organic substrates adsorbed on the surface of photocatalyst [5,6]. The semiconductor materials such as undoped titanium dioxide nanoparticles (UTDONPs) have been used for the

* Corresponding author.

elimination of toxic emerging contaminants present in the aquatic environment due to its specific features. UTDONPs are cheaper, stable and effective to eliminate toxic emerging contaminants. Preparation of RuO_2/TiO_2 mesoporous heterostructures and their enhanced photocatalytic properties for the photodecomposition of emerging organic contaminants are reported in the literature [7–9]. The properties of UTDONPs can be modified by doping a foreign material into its crystal lattice which reduces the particle size and increases the photocatalytic activity of semiconductor photocatalyst. The transition metal ruthenium can be doped into the crystal lattice of UTDONPs due to a slightly smaller atomic radius of ruthenium (0.056 nm) than titanium (0.060 nm) [10]. This doping of ruthenium in UTDONPs reduces the rate of wasteful recombination of photo-generated electron-hole pair and hence increases the rate of mineralization of organic contaminants adsorbed on the surface of photocatalyst [11,12]. The bandgap energy of ruthenium doped titanium dioxide nanoparticles (RDTDONPs) is smaller than UTDONPs. The rate of mineralization of organic contaminants by RDTDONPs is higher due to more number of surface defects observed in photocatalyst [13].

Zidovudine (ZDV) (Fig. 1) is used as a model compound mixed with the double-distilled water for this investigation. It is the first antiretroviral drug used for treating Acquired Immune Deficiency Syndrome (AIDS) [14]. A literature survey reveals the presence of antiretroviral drugs in the aquatic environment. The molecular mass of ZDV is 267.24 g mol^{-1} [15]. A literature survey shows that there are no studies found on the mineralization of organic substrate ZDV by RDTDONPs under UV illumination. Hence, a detailed study was undertaken to eliminate organic contaminant ZDV with the help of RDTDONP by varying different parameters. Photo-degraded products of ZDV were analysed. A suitable mechanism is proposed in agreement with the experimental results and kinetic data.

2. Experiments and materials

2.1. Chemical reagents

The model compound pharmaceutical drug ZDV was obtained Sigma-Aldrich (Bengaluru, India) and its freshly prepared stock solution in double-distilled water were used for the investigation. The semiconductor photocatalyst RDTDONPs of different mole ratio 0.2%, 0.4%, 0.6%, and 0.8% were synthesized in the laboratory with the help of $RuCl_3{\cdot}3H_2O$ and TiO_2 (anatase form). Acetate, phosphate and borate buffers were prepared to maintain acidic, neutral and alkaline conditions.

2.2. Instruments and methods

The pH was recorded with the help of Elico pH meter (models LI 120, Hyderabad, India). The characterisation of semiconductor photocatalysts was carried out with the help of sophisticated methods such as Siemens X-ray diffractometer (Texas, USA) (XRD) (Cu source) AXS D5005, scanning electron microscopy (SEM) JEOL JSM 6360 (Peabody, USA), energy-dispersive X-ray (EDX) spectroscopy and transmission electron microscopy (TEM) JEOL JEM-2010. The surfaces of UTDONPs and RDTDONPs were illuminated with UV light intensity = 4 mW cm^{-2} inside the UV cabinet (Mercury lamp, PHILIPS (Mumbai, India), TUV 8W T5, E_{max} = 254 nm) to generate powerful hydroxyl free radicals for the complete mineralization of ZDV. The UV light intensity which was used for the illumination of the photocatalyst was recorded using an optical power meter (Newport 2936 - C). The kinetic investigation was performed with the help of A CARY 50 Bio UV-VIS spectrophotometer (Varian BV, The Netherlands) with a temperature controller to record the absorbance of the reaction mixture. The analysis and identification of different photo-degraded products of substrate ZDV were performed using a high-resolution mass spectrophotometer (HR-MS) (Thermo Scientific Q Exactive, Waltham, United States) with Column-Thermo Scientific Hypersil Gold C18 (Waltham, United States) (dimension 150 × 4.6 mm–8 μm) and high-performance liquid chromatography (Shimadzu Prominence, Kyoto, Japan). Rate constants were found reproducible within the error margin of ±7%. The semiconductor photocatalysts were dispersed in a suitable solvent ultrasonically and dropped on a copper grid. After drying, the photocatalyst material was used for the characterisation by TEM. Bandgap measurement of photocatalyst was done with the help of Fourier transform infrared (FTIR) PerkinElmer model-spectrum 100 (Bridgeport Avenue Shelton, CT 06484-4794 USA).

2.3. Synthesis of photocatalysts by liquid impregnation method

0.2%, 0.4%, 0.6%, and 0.8% (mole ratio) RDTDONPs are synthesized with the help of liquid impregnation method by adding an appropriate quantity of $RuCl_3 3H_2O$ in 100 mL of 0.2 M HCl solution. Thereafter, 1.0 g of titanium dioxide nanoparticles (anatase) was added into the reaction mixture. Subsequently, this mixture was stirred continuously for a period of 5 h and left untouched for 20 h to settle down. Further, the slurry was placed in an oven at a constant temperature of 85°C for 15 h to convert it into dried form. Then, the dried solids were grounded with the help of mortar and pestle. The process of calcination was carried out at 400°C in a muffle furnace (heating rate is 10°C/min) for 3 h. The temperature in a muffle furnace should not be higher than 400°C to avoid the conversion of TiO_2 (anatase) into TiO_2 (rutile) [16].

2.4. Photocatalytic degradation of substrate ZDV under UV illumination

This process of photo-degradation was initiated by adding appropriate concentrations of organic substrate

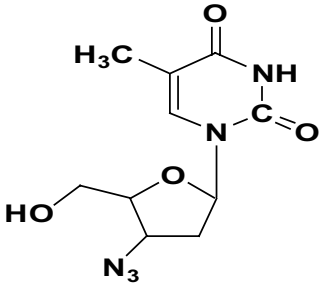

Fig. 1. Chemical structure of ZDV.

ZDV and a suitable buffer into a Pyrex beaker. Thereafter, a dosage of 0.10 g L^{-1} RDTDONPs was added into a Pyrex beaker. This reaction mixture was left untouched for the period of 3 h in a dark room to establish the equilibrium of adsorption and desorption between the semiconductor RDTDONPs and organic substrate ZDV. Subsequently, this reaction mixture was placed on a magnetic stirrer for nonstop stirring and the surface of the photocatalyst was irradiated with 8 W UV-lamp (Phillips) at 254 nm. Thereafter, the small quantity of this photo-degraded mixture was transferred for the centrifugation process at regular intervals. The centrifugation of reaction mixture was carried out at 5,000 revolutions per minute for 15 min. Subsequently, this reaction mixture was transferred into cuvette to monitor the decrease in the absorbance at 267 nm with the help of a spectrophotometer. Then, the photo-degraded mixture was filtered properly and used for the analysis of photo-degraded products of ZDV with the help of HR-MS. The verification of Lambert-Beers law was performed by changing the [ZDV] from 1.0×10^{-6} to 1.0×10^{-5} mol L^{-1} at 267 nm. The pseudo-first-order rate constants were determined from the plot of log absorbance vs. time.

3. Results and discussion

3.1. Comparison of different treatments for the mineralization of ZDV

Experimental results show that the rates of mineralization of ZDV with modified RDTDONPs under UV illumination are higher than UV and UV/UTDONPs as presented in Fig. 2.

Kinetic data shows that the rate of mineralization of substrate ZDV is higher using 0.8% (mole ratio) RDTDONPs than 0.2%, 0.4%, and 0.6% (mole ratio) RDTDONPs as presented in Fig. 3. This may be due to a decrease in particle size, increase in surface area and enhancement in the photocatalytic activity of the photocatalyst 0.8% (mole ratio) RDTDONPs. 0.8% (mole ratio) RDTDONPs enhances the surface charge transfer, increases surface reactivity and decelerates the wasteful recombination of photo-generated electron-hole pair [17]. It is also observed from the kinetic data that the rate of mineralization of ZDV is found to be decreased beyond 0.8% (mole ratio) RDTDONPs. This may due to the accumulation of ruthenium metal on the photocatalyst surface and not entering into the crystalline structure of photocatalyst.

Experimental results show that the percentage degradation efficiency of ZDV with UV, UV/UTDONPs, 0.2%,0.4%, and 0.8% (mole ratio) RDTDONPs are found to be 50%, 62%, 75%, 82%, and 96% respectively as presented in Fig. 4.

This indicates that percentage degradation efficiency of ZDV is higher with 0.8% (mole ratio) RDTDONPs treatment as compared to other treatments in 100 min at fixed reaction conditions [ZDV] = 1×10^{-5} mol L^{-1}, [Photocatalyst] = 100 mg L^{-1}, light intensity = 4 mW cm^{-2} and pH = 4. The percentage degradation efficiency of ZDV moiety in dark was found to be very low.

3.2. Characterization of UTDONPs and RDTDONPs photocatalysts

3.2.1. XRD analysis and Scherrer equation

The particle size and phase purity of UTDONPs and 0.2%, 0.4%, and 0.8% (mole ratio) RDTDONPs were studied and determined with the help of XRD pattern using Cu K_α radiation over a scan range of 2θ (0°–90°). XRD

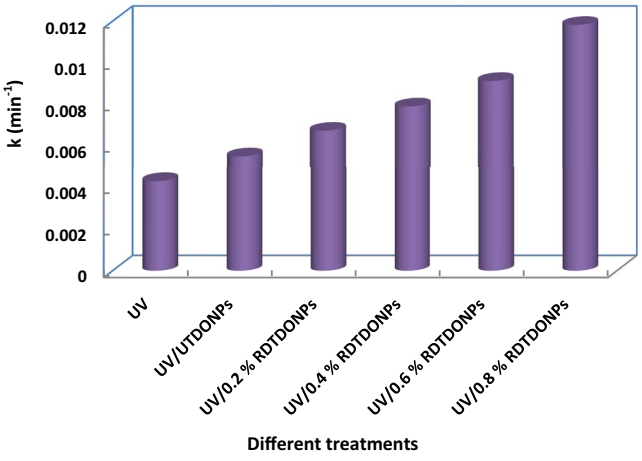

Fig. 2. Rate constants for the mineralization of substrate ZDV by various treatments.

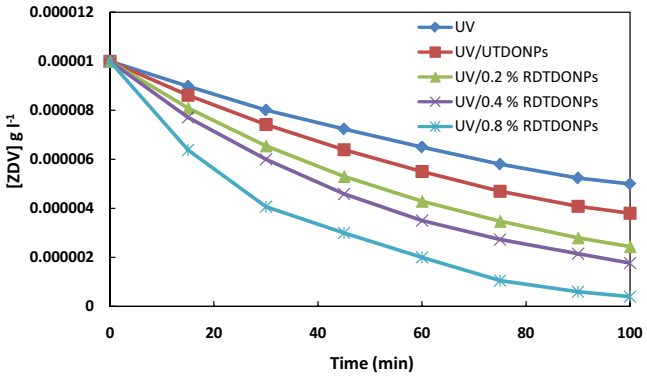

Fig. 3. The plot of [ZDV] vs. time (min) using UV, UV/UTDONPs and modified RDTDONPs.

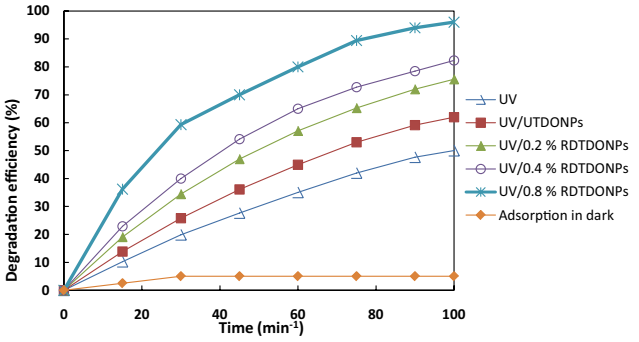

Fig. 4. Percentage degradation efficiency by different treatments with time.

pattern shows well-defined reflections for all 10 peaks of UTDONPs and RDTDONPs from crystal planes. XRD pattern does not show an additional peak associated with secondary phases of photocatalysts. This observation confirms the proper doping of ruthenium into the interstitial position of the crystal lattice of the photocatalyst. It means that the anatase form of photocatalyst is not disturbed by doping 0.2%, 0.4%, and 0.8% (mole ratio) of ruthenium metal into the crystal structure. This shows that the photocatalysts are in a single phase. XRD shows 10 peaks at crystal planes (101), (004), (200), (105), (211), (204), (116), (220), and (215), (224) of photocatalyst over a scan range of 2θ (0°–90°) as reported in our earlier investigation [6]. Scherrer Eq. (1) was applied to determine the average particle size of UTDONPs and modified RDTDONPs from a full-width half-maximum of a (101) peak of photocatalyst [18].

$$D = \frac{k\lambda}{\beta\cos\theta} \tag{1}$$

D (the average crystalline diameter) can be calculated by substituting the values for different terms such as λ (X-ray wavelength = 0.154 × 10^{-9} m), k (dimensionless shape factor = 0.94), θ (Bragg diffraction angle from XRD pattern) and β (full width at half – maximum from XRD pattern) in Eq. (1). The calculated average particle size from Scherrer equation were found to be 17.05 nm for UTDONPs, 16.74 nm for 0.2% (mole ratio) RDTDONPs, 15.67 nm for 0.4% (mole ratio) RDTDONPs, and 14.38 nm for 0.8% (mole ratio) RDTDONPs. The smaller average particle size in 0.8% (mole ratio) RDTDONPs shows the increase in the rate of mineralization of substrate ZDV due to the enhancement of photocatalytic activity and surface area.

3.2.2. SEM analysis for UTDONPs and 0.8% (mole ratio) RDTDONPs

UTDONPs and 0.8% (mole ratio) RDTDONPs were characterized with the help of JEOL JSM 6360 SEM to study the morphologies of photocatalysts. SEM images were obtained at higher magnification (15,000×), precision distance (1-micrometer length) and applied voltage (20 kV). SEM micrograph of 0.8% (mole ratio) RDTDONPs shows a porous and spongy network of unequal shapes. SEM micrograph of 0.8% (mole ratio) RDTDONPs is reported in our previous investigation [6]. This enhances the photocatalytic activity and surface area of 0.8% (mole ratio) RDTDONPs which accelerates the rate of mineralization of ZDV into harmless products. It is also observed from the SEM image of 0.8% (mole ratio) RDTDONPs that ruthenium metal is not equally decorated on the photocatalyst surface [18].

3.2.3. EDX analysis for UTDONPs and 0.8% (mole ratio) RDTDONPs

The quantitative element analysis of UTDONPs and 0.8% (mole ratio) RDTDONPs was performed by EDX JEOL JED-2300 and was reported in our earlier work of photocatalytic degradation of Linezolid by 0.8% (mole ratio) RDTDONPs [6]. There are two and three peaks observed in the EDX of photocatalyst UTDONPs and 0.8% (mole ratio) RDTDONPs respectively. The atomic percentage of titanium, oxygen and ruthenium as shown by the EDX spectrum are 36.42, 62.78, and 0.80 respectively. This non-stoichiometric ratio of three elements observed in photocatalyst 0.8% (mole ratio) RDTDONPs enhances the photocatalytic activity and rate of photo-degradation of substrate ZDV [19]. EDX spectrum of 0.8% (mole ratio) RDTDONPs related with O Kα, Ru Kα, and Ti Kα confirms the presence of only three elements (Ti, O and Ru) and hence no other impurity is observed.

3.2.4. TEM analysis for 0.8% (mole ratio) RDTDONPs at 100 nm and 20 nm resolutions

TEM JEOL JEM-2010 was used to investigate the particle size and morphology of 0.8% (mole ratio) RDTDONPs photocatalyst which was synthesized by the Liquid Impregnation method. TEM micrographs of 0.8% (mole ratio) RDTDONPs photocatalyst at 100 nm and 20 nm resolutions (inset SAED pattern) are presented in our earlier study [6]. TEM micrographs of 0.8% (mole ratio) RDTDONPs photocatalyst show that the particles are found to be well crystallized uniformly dispersed aggregates and rod shape without any defects. TEM micrographs show the mean diameter of 0.8% (mole ratio) RDTDONPs from 15 to 20 nm. This average diameter of the photocatalyst is found closer to the values obtained from the X-ray line broadening of XRD spectra. TEM micrographs show doping of 0.8% (mole ratio) ruthenium into interstitial positions of the crystal structure due to the smaller size of ruthenium than titanium.

3.2.5. FTIR spectra of UTDONPs and RDTDONPs

Analysis of FTIR spectra of UTDONPs and modified RDTDONPs indicates a broad bandgap (3,500 to 3,000 cm^{-1}) for the characteristic band of OH groups. It is also observed from the FTIR spectra of photocatalysts that peak at 1,635 is related to the stretching vibration of the OH group and indicating H_2O as moisture [20]. Further analysis of FTIR spectra shows the peak between 750 to 500 cm^{-1} is related to Ti–O stretching bands present in the photocatalysts. FTIR spectra show a strong band (800 to 450 cm^{-1}) associated with the calcination of the synthesized photocatalysts UTDONPs and RDTDONPs in a muffle furnace (heating rate is 10°C/min) [10,21].

3.2.6. Measurement of band gaps of photocatalysts RDTDONPs

Measurement of band gaps of photocatalysts RDTDONPs were carried out with the help of a PerkinElmer Lambda 950 UV/Vis/NIR spectrophotometer having a 150 mm integrating sphere attachment. Barium sulphate was used as a reflectance standard to record diffuse reflectance in the range from 800 to 200 nm of modified RDTDONPs. Diffuse reflectance spectra were used to calculate the optical band gaps (E_g) of modified semiconductor RDTDONPs from the Tauc plot of the Kubelka-Munk function which is shown with the help of Eq. (2).

$$F(R) = \frac{(1-R)^2}{2R} \tag{2}$$

In Eq. (2), the term R denotes the diffuse reflectance of the photocatalyst. The optical band gaps for modified semiconductor RDTDONPs are calculated from the plot of $[F(R)\ h\upsilon]^{1/2}$ vs. the photon energy ($h\upsilon$) curve by extrapolating the linear portion of the modified Kubelka-Munk function on the zero ordinate [10]. In this case, the direct application of the Tauc method has resulted from the inaccurate estimation of bandgap energy. It is difficult to split the Kubelka-Munk spectrum into individual components. Hence, a baseline approach is applied to estimate the bandgap energies of modified semiconductor photocatalysts [22]. The linear fit of the fundamental peak is applied as per the Tauc method. Additionally, a linear fit is used as an abscissa for the slope below the fundamental absorption. As per the baseline approach, the accurate bandgap energies are estimated from the intersection of two fitting lines for the modified semiconductor photocatalysts. These estimated bandgap energies as per baseline approach for 0.2%, 0.4%, and 0.8% (mole ratio) RDTDONPs are 3.13, 3.09, and 3.02 eV respectively. These values of band gaps are found smaller for RDTDONPs as compared to UTDONPs (bandgap 3.22 eV) as reported in the previous studies. This bandgap measurement data confirms the proper doping of ruthenium metal into the crystal lattice of photocatalyst [23].

3.2.7. Measurement of surface area of photocatalysts UTDONPs and RDTDONPs

The rate of mineralization of substrate ZDV is related to the surface area of photocatalysts. Therefore, it is very crucial to find out the surface area of semiconductor photocatalysts UTDONPs and modified RDTDONPs. The measurement of surface area was performed by Brunauer–Emmett–Teller nitrogen gas adsorption method and smart instruments surface area analyser (Smart Sorb 92/93). The surface area of semiconductor photocatalysts UTDONPs, 0.2%, 0.4%, and 0.8% (mole ratio) RDTDONPs are found to be 85.19, 88.82, 92.97, and 94.31 m^2/g respectively. The reason behind the a decrease in particle size can be understood with the help of Nae-Lih Wu's theory [10]. This theory elucidates that decrease in particle size of the modified photocatalyst is due to an interaction on the boundaries between titanium dioxide nanoparticles and ruthenium. This causes the restriction on the motion of crystallites. As a result of this, the specific area of modified photocatalyst increases with a decrease in the size of the nanoparticles. Hence, the increase in surface area of 0.8% (mole ratio) RDTDONPs enhances the photocatalytic activity and rate of mineralization of ZDV moiety.

3.3. Influence of loading of semiconductor photocatalysts on the rate of mineralization of ZDV

The influence of UTDONPs and 0.8% RDTDONPs on the rate of mineralization of ZDV was performed by varying the photocatalyst dosage from 0.05 to 0.250 g L^{-1} into the reaction mixture which is kept inside the UV cabinet at fixed [ZDV] = 1×10^{-5} mol L^{-1}, UV light intensity = 4 mW cm^{-2} and pH = 4. It is observed from the kinetic data that the rate of mineralization of ZDV accelerates with an increase in photocatalyst dosage from 0.05 to 0.1 g L^{-1} as presented in Fig. 5. This increase in the rate of mineralization of ZDV

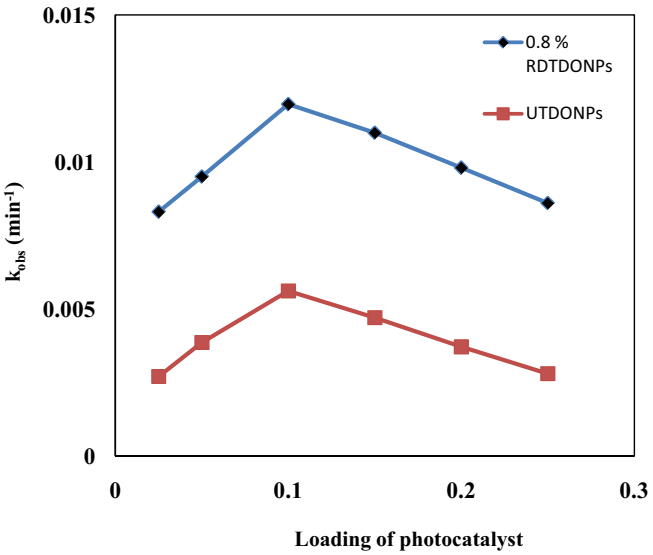

Fig. 5. Effect of loading of different quantities of photocatalysts UTDONPs and 0.8% (mole ratio) RDTDONPs at [ZDV] = 1×10^{-5} mol L^{-1}, UV light intensity = 4 mW cm^{-2} and pH = 4.

by photocatalyst dosage from 0.05 to 0.1 g L^{-1} may be due increase in exposed surface area and active sites of UTDONPs and RDTDONPs for the adsorption of substrate ZDV molecules. There is an increase in the powerful hydroxyl species to mineralize the substrate ZDV molecules into harmless products. This is also supported by previous investigations [10]. It is also interesting to note that the further addition of photocatalyst dosage beyond 0.1 g L^{-1} decelerates the rate of mineralization of substrate ZDV. This decrease in the rate of mineralization of ZDV beyond the limiting value of 0.1 g L^{-1} of photocatalyst dosage maybe because there is an increase in turbidity into the beaker placed inside the UV cabinet and inhibits the photon energy to produce more number of powerful hydroxyl species [24–26].

3.4. Effect of variation in concentration of substrate ZDV

The rate of photocatalytic degradation of ZDV moiety was investigated by varying the concentration of ZDV moiety from 2.0×10^{-6} to 2.0×10^{-5} mol L^{-1} at fixed conditions such as the concentration of photocatalyst 0.8% (mole ratio) RDTDONPs = 1 g L^{-1}, UV light intensity = 4 mW cm^{-2} inside the UV cabinet and pH = 4. Experimental results show that the rate of photocatalytic degradation of substrate ZDV was found to be increased with an initial increase in the concentration of substrate ZDV at fixed conditions as presented in Fig. 6 for UV, UV/UTDONPs and UV/0.8% (mole ratio) RDTDONPs treatments. This can be attributed to the fact that as the concentration of ZDV increases from 2.0×10^{-6} to 1.0×10^{-5} mol L^{-1}, there may be a higher rate of adsorption of a large number of exciting ZDV molecules on the surface of photocatalyst 0.8% (mole ratio) RDTDONPs. The kinetic data also reveals that the rate of photocatalytic degradation of substrate ZDV reaches a maximum at [ZDV] = 1.0×10^{-5} mol L^{-1}. Thereafter, it is observed that the rate of photocatalytic degradation of ZDV declines beyond

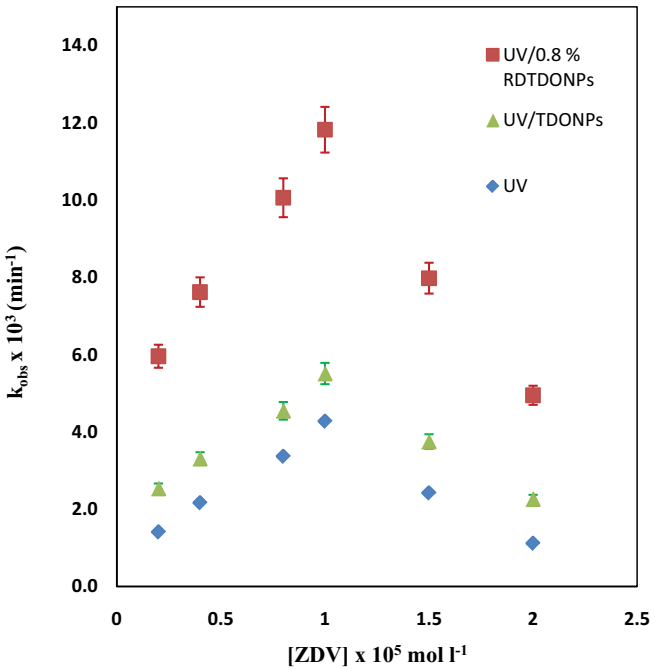

Fig. 6. Effect of varying [ZDV] from 2 × 10^{-6} to 2 × 10^{-5} mol L^{-1} on the rate of photodegradation of ZDV by UV, UV/UTDONPs and UV/0.8% (mole ratio) RDTDONPs.

the higher concentration 1.0 × 10^{-5} mol L^{-1} of substrate ZDV due to very large number of ZDV molecules which works as a filter and hence it prevents the light photons from illuminating the surface of photocatalyst. As a result of this, there is no further increase in photo-generated hydroxyl free radicals and superoxide radical anions [24].

3.5. Adsorption capacities at different pH of reaction mixture

The adsorption efficiency at different pH values (4.0 to 8.0) is evaluated by changing the concentration of substrate ZDV moiety in the range 2.0 × 10^{-6} to 1.0 × 10^{-5} mol L^{-1} and UV light intensity = 4 mW cm^{-2} inside the UV cabinet. 10 mg of photocatalyst 0.8% (mole ratio) RDTDONPs was mixed in100 mL beaker containing a suitable quantity of substrate ZDV solution placed inside the UV cabinet. Thereafter, the particular pH conditions (acidic, neutral and alkaline) of reaction mixtures were adjusted and recorded using Elico pH meter. This reaction mixture was sealed and continuously stirred at a temperature of 25°C for a period of 12 h in a dark room. Subsequently, this reaction mixture was placed in a centrifuge machine for 10 min. Thereafter, the absorbance of the supernatant was recorded with the help of a spectrophotometer. The adsorption capacity (S) was evaluated with the help of Eq. (3).

$$S = \frac{(C - C_0)V}{m} \tag{3}$$

By putting the values for different terms such as C_0 (Initial concentration of substrate ZDV moiety in mol L^{-1}), C (Equilibrium concentration of substrate ZDV moiety in mol L^{-1}), V (Volume of the reaction mixture in l) and m (Amount of photocatalyst 0.8% mole ratio RDTDONPs in g) in the above Eq. (3), adsorption capacities at different pH of the reaction mixture were evaluated and listed in Table 1. Experimental results show that adsorption capacities are higher in acidic conditions than the basic condition of the reaction mixture.

The phenomenon of adsorption of substrate ZDV molecules on the surface of RDTDONPs was carried out by placing the reaction mixture in a dark room with continuous stirring in a beaker using a magnetic stirrer for overnight by adding different quantities of photocatalyst 0.8% (mole ratio) RDTDONPs. Thereafter, this reaction mixture was centrifuged in a centrifuge tube for 10 min and recorded the concentration of the supernatant. The experimental result indicates that there was no considerable loss of substrate ZDV at the surface of photocatalyst. Therefore, the phenomenon of adsorption has no significant effect on the degradation rate of ZDV in the absence of UV light [10].

3.6. Effect of pH on the rate of mineralization of substrate ZDV molecules by photocatalyst

The pH of the medium affects the adsorption capacity and surface properties of the semiconductor 0.8% (mole ratio) RDTDONPs. The effect of variation in pH (4.0–8.0) of the medium on the rate of mineralization of ZDV moiety was carried out by keeping the concentration of 0.8% (mole ratio) RDTDONPs = 1 g L^{-1}, [ZDV] = 1 × 10^{-5} mol L^{-1} and UV lamp light intensity = 4 mW cm^{-2} fitted inside the UV cabinet. The kinetic measurement indicates that the rate of mineralization of ZDV by photocatalyst is found to be accelerated in acidic conditions as presented in Fig. 7. This may be because the positively charged surface of photocatalyst 0.8% (mole ratio) RDTDONPs adsorbs more negatively charged ZDV ions on its surface in acidic medium. Ru-$TiOH_2^+$ is found to be a major active species in acidic medium (pH 4.0 to 6.0). Due to this, there is an increase in a number of effective collisions between ZDV moiety and semiconductor 0.8% (mole ratio) RDTDONPs and hence the rate of mineralization of ZDV by photocatalyst is found higher in acidic medium. The rate of mineralization of ZDV by photocatalyst decelerates in alkaline conditions. This may be because negatively charged hydroxyl ions are accumulated on the surface of photocatalyst 0.8% (mole ratio) RDTDONPs in the alkaline condition of the reaction mixture. Consequently, the repulsive forces between negatively

Table 1
Adsorption capacities with different pH of reaction mixtures at [ZDV] = 1 × 10^{-1} mol L^{-1}, 0.8% (mole ratio) RDTDONPs = 100 g L^{-1}, pH = 4 and UV light intensity = 4 mW cm^{-2}

pH of reaction mixtures	Adsorption capacities (mol g^{-1})
4.0	0.00093
5.0	0.00085
6.0	0.00077
7.0	0.00071
8.0	0.00062

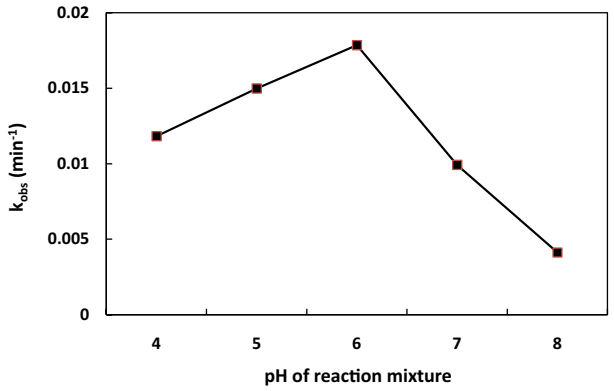

Fig. 7. Effect of variation in pH on the rate of mineralization of ZDV with 0.8% (mole ratio) RDTDONPs = 1 g L^{-1}, [ZDV] = 1 × 10^{-5} mol L^{-1} and UV lamp light intensity = 4 mW cm^{-2}.

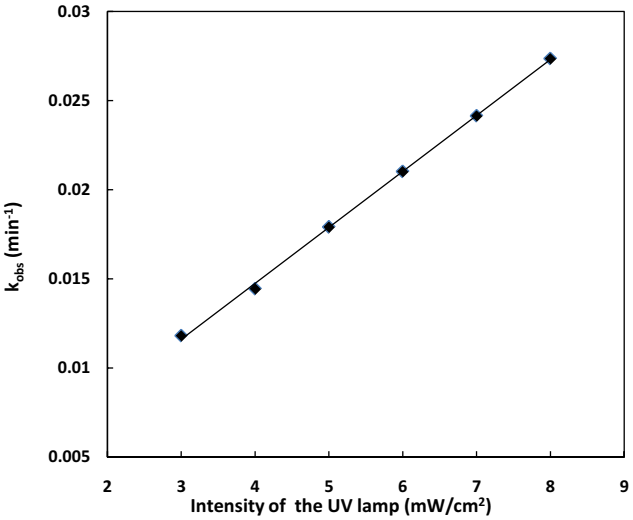

Fig. 8. Effect of variation in light intensity on the rate of mineralization of ZDV with 0.8% (mole ratio) RDTDONPs = 1 g L^{-1}, [ZDV] = 1 × 10^{-5} mol L^{-1} and pH = 4.

charged ZDV ions and negatively charged hydroxyl ions enhance in alkaline conditions. Ru-TiO^- is found to be major active species in basic medium (pH 7.0 to 8.0). Therefore, the rate of mineralization of ZDV molecules by 0.8% (mole ratio) RDTDONPs is higher in acidic conditions as compared to the basic condition [27–29]. The experimental data indicate that the adsorption capacity of the photocatalyst is higher in acidic medium in comparison to the alkaline medium. ZDV interacts with hydrogen and hydroxyl ions which results in ZDV° (neutral) and ZDV^- (anion). ZDV° (neutral) species are adsorbed more on the surface of photocatalyst RDTDONPs in acidic conditions as compared to highly ionized species. ZDV^- (anion) species dominates in alkaline medium at higher pH and consequently hampers the adsorption of substrate species on the surface of photocatalyst RDTDONPs due to electrostatic repulsive forces. On the other hand, the adsorption of ZDV° (neutral) species on the surface of RDTDONPs in alkaline medium may be due to weak van der Waals forces of attraction. It is well supported by previous investigations [30].

3.7. UV light intensity effect on the rate of mineralization of ZDV moiety

UV light intensity effect on the rate of mineralization of ZDV moiety by photocatalyst RDTDONPs was performed by altering the distance of UV lamp (Mercury lamp, PHILIPS (Mumbai, India), TUV 8W T5, E_{max} = 254 nm) from the beaker placed inside the UV cabinet to generate powerful hydroxyl free radicals for the complete mineralization of substrate ZDV. The UV light intensity which was used for the illumination of photocatalyst RDTDONPs was recorded with the help of Newport 2936-C, Deere Avenue Irvine, California 92606.. The kinetic data shows that the rate of mineralization of substrate ZDV moiety enhances with an increase in UV light intensity (Fig. 8). The reason behind this may be that there is an increase in a number of photons striking the per unit area of 0.8% (mole ratio) RDTDONPs which consequently enhances the photo-generated electron-hole pairs. The photo-generated holes at the surface of photocatalyst 0.8% (mole ratio) RDTDONPs mineralize adsorbed ZDV moiety effectively into harmless products [31].

3.8. Photo-degradation electron-hole pair mechanism of ZDV with 0.8% (mole ratio) RDTDONPs

The surface of photocatalyst 0.8% (mole ratio) RDTDONPs was irradiated with UV light of appropriate intensity to produce electron-hole pairs for the mineralization of substrate ZDV into harmless products [32]. Most of these photo-generated electron-hole pairs present on the surface of photocatalyst 0.8% (mole ratio) RDTDONPs undergo wasteful recombination. Redox reactions are initiated by non-combined photo-generated electron-hole pairs on the surface of photocatalyst 0.8% (mole ratio) RDTDONPs to mineralize ZDV into harmless products [29]. There are various reactions taking place at the valence and conduction bands of the photocatalyst 0.8% (mole ratio) RDTDONPs.

$$\text{RDTDONPs} + h\nu \rightarrow \text{RDTDONPs}\ (h^+ + e^-) \quad (4)$$

Reactions at the valence band: photo-generated holes (RDTDONPs) h^+ generated at the surface of photocatalyst reacts with H_2O molecules and forms hydroxyl free radicals ($^\bullet OH$) as shown in Eq. (5).

$$(\text{RDTDONPs})\ h^+ + H_2O \rightarrow H^+ + {}^\bullet OH \quad (5)$$

Strong hydroxyl free radicals ($^\bullet OH$) mineralize the substrate ZDV moiety into harmless photo-degraded products [10,29,33].

$$\text{ZDV} + {}^\bullet OH \rightarrow \text{Photo-degraded harmless products} \quad (6)$$

Reactions at the conduction band: photo-generated electrons (RDTDONPs) e^- interacts with oxygen molecules at the surface of photocatalyst 0.8% (mole ratio) RDTDONPs and produces superoxide radical anions ($^\bullet O_2^-$). The formation of superoxide radical anions would be possible due to the transfer of trapped e^- from the surface of ruthenium metal to

oxygen atom [34]. As a result of this, the wasteful recombination of (RDTDONPs) h^+ and (RDTDONPs) e^- is prevented. This enhances the rate of mineralization of substrate ZDV moiety into harmless photo-degraded products using the photocatalyst 0.8% (mole ratio) RDTDONPs.

$$(\text{RDTDONPs})\ e^- + O_2 \rightarrow {}^{\bullet}O_2^- \quad (7)$$

Thereafter, ${}^{\bullet}O_2^-$ reacts with H^+ to form $HO_2^{\bullet}$ free radicals at the surface of semiconductor photocatalyst.

$${}^{\bullet}O_2^- + H^+ \rightarrow HO_2^{\bullet} \quad (8)$$

Subsequently, these free radicals interact with (RDTDONPs) e^- at the conduction band of the photocatalyst and forms HO_2^- species [35,36].

$$HO_2^{\bullet} + (\text{RDTDONPs})\ e^- \rightarrow HO_2^- \quad (9)$$

The powerful oxidizing agent H_2O_2 is formed at the conduction band of photocatalyst due to the interaction between HO_2^- anion and H^+ ions.

$$HO_2^- + H^+ \rightarrow H_2O_2 \quad (10)$$

Thereafter, H_2O_2 interacts with (RDTDONPs) e^- at the conduction band of the photocatalyst to generate powerful hydroxyl species (${}^{\bullet}OH$).

$$H_2O_2 + (\text{RDTDONPs})\ e^- \rightarrow OH^- + {}^{\bullet}OH \quad (11)$$

Subsequently, these powerful hydroxyl species (${}^{\bullet}OH$) mineralizes the substrate ZDV moiety at the conduction band into photo-degraded harmless products [10,33,37].

$${}^{\bullet}OH + \text{ZDV} \rightarrow \text{Photo-degraded harmless products} \quad (12)$$

This photo-degradation of substrate ZDV moiety on the surface of photocatalyst 0.8% (mole ratio) RDTDONPs takes place due to dissolved O_2 and H_2O molecules as per the plausible mechanism. The formation of ${}^{\bullet}OH$ species and photo-degradation of substrate ZDV moiety would have not been possible without O_2 and H_2O molecules [6,29].

Three photo-degraded products of ZDV are identified over the mass range 100–800 m/z and labeled as ZDV_P1, ZDV_P2 and ZDV_P3. These UV degraded products of ZDV along with their structures and names are presented in Fig. 9 and listed in Table 2.

Three UV degraded products of ZDV were analysed and identified by positive mode electrospray ionization (ESI^+) technique using HR-MS over the mass range 100–800 m/z. The mass spectra of standard ZDV and photo-degraded ZDV are presented in Figs. 10a and b.

The photocatalytic degradation of substrate ZDV moiety adsorbed on the surface of 0.8% (mole ratio) RDTDONPs is presented in Fig. 11 using kinetic data, experimental results and HR-MS analysis.

4. Conclusion

A suitable photo-generated electron-hole pair mechanism is proposed in agreement with kinetic data and experimental

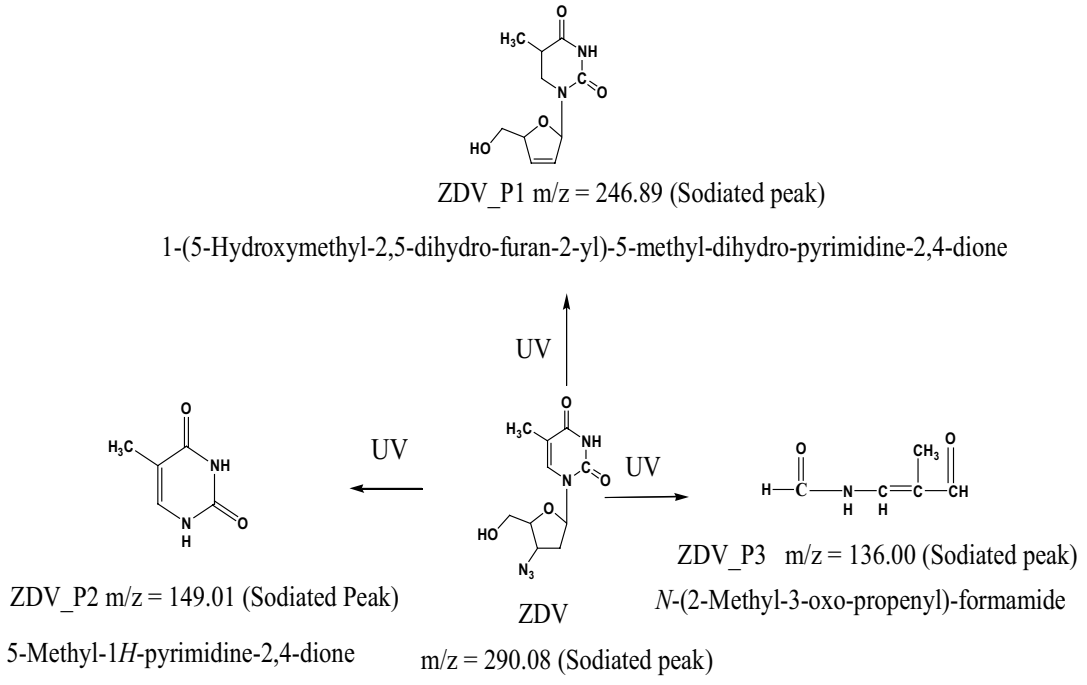

Fig. 9. Photo-degraded products of substrate ZDV under UV illumination at 254 nm.

Table 2
Photo-degraded products of substrate ZDV with the help of HR-MS analysis

ZDV Products	Measured $M+H^+/M+Na^+$	Theoretical mass (Da)	Molecular formula	Name of the identified photo degraded products of substrate ZDV
ZDV_P1	246.89	224.21	$C_{10}H_{12}N_2O_4$	1-(5-Hydroxymethyl-2,5-dihydro-furan-2-yl)-5-methyl-1H-pyrimidine-2,4-dione
ZDV_P2	149.01	126.11	$C_5H_6N_2O_2$	5-Methyl-1H-pyrimidine-2,4-dione
ZDV_P3	136.00	113.11	$C_5H_7NO_2$	N-(2-Methyl-3-oxo-propenyl)-formamide

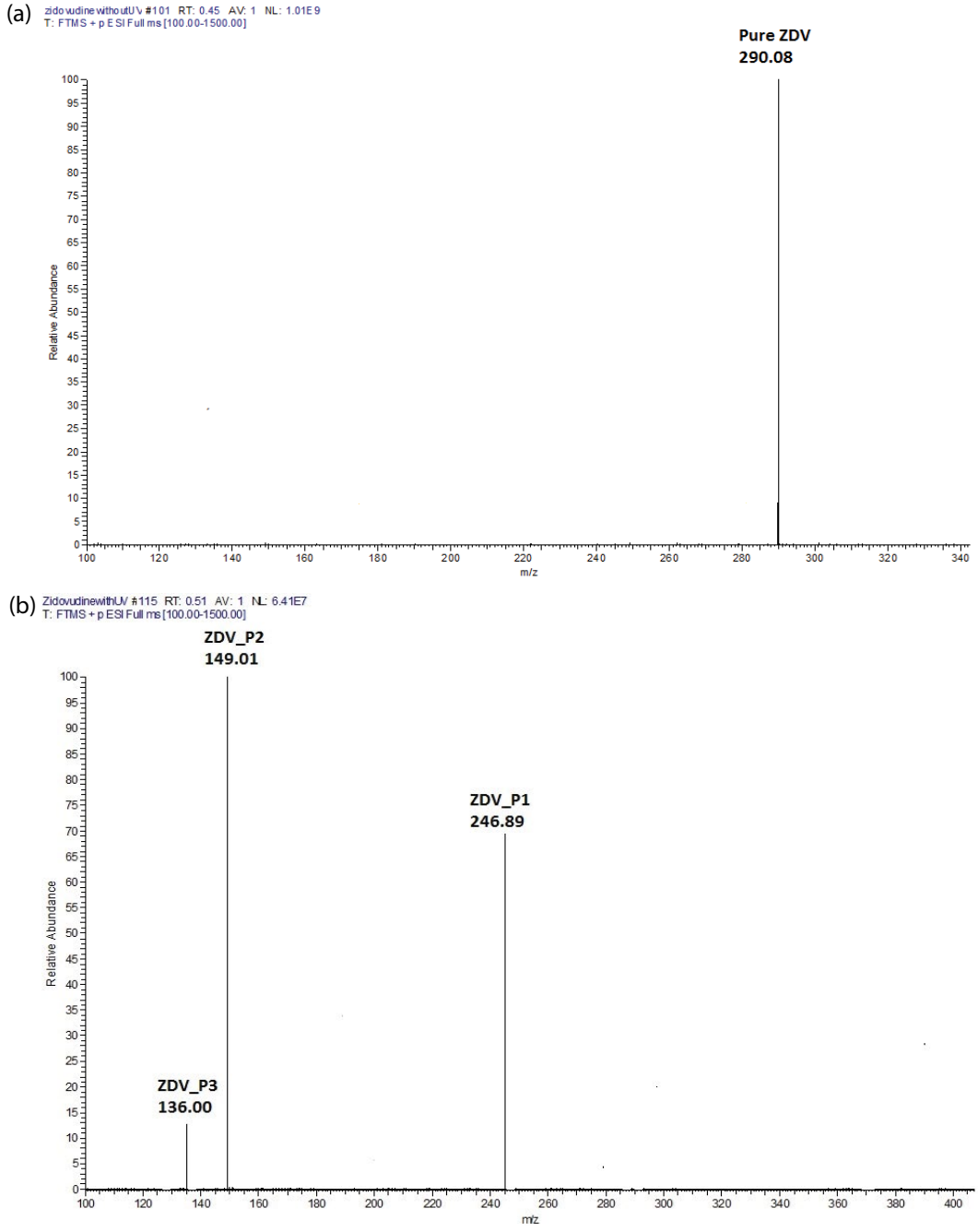

Fig. 10. (a) Mass spectra of pure substrate ZDV moiety using HR-MS and (b) mass spectra of three identified UV degraded products of substrate ZDV using HR-MS.

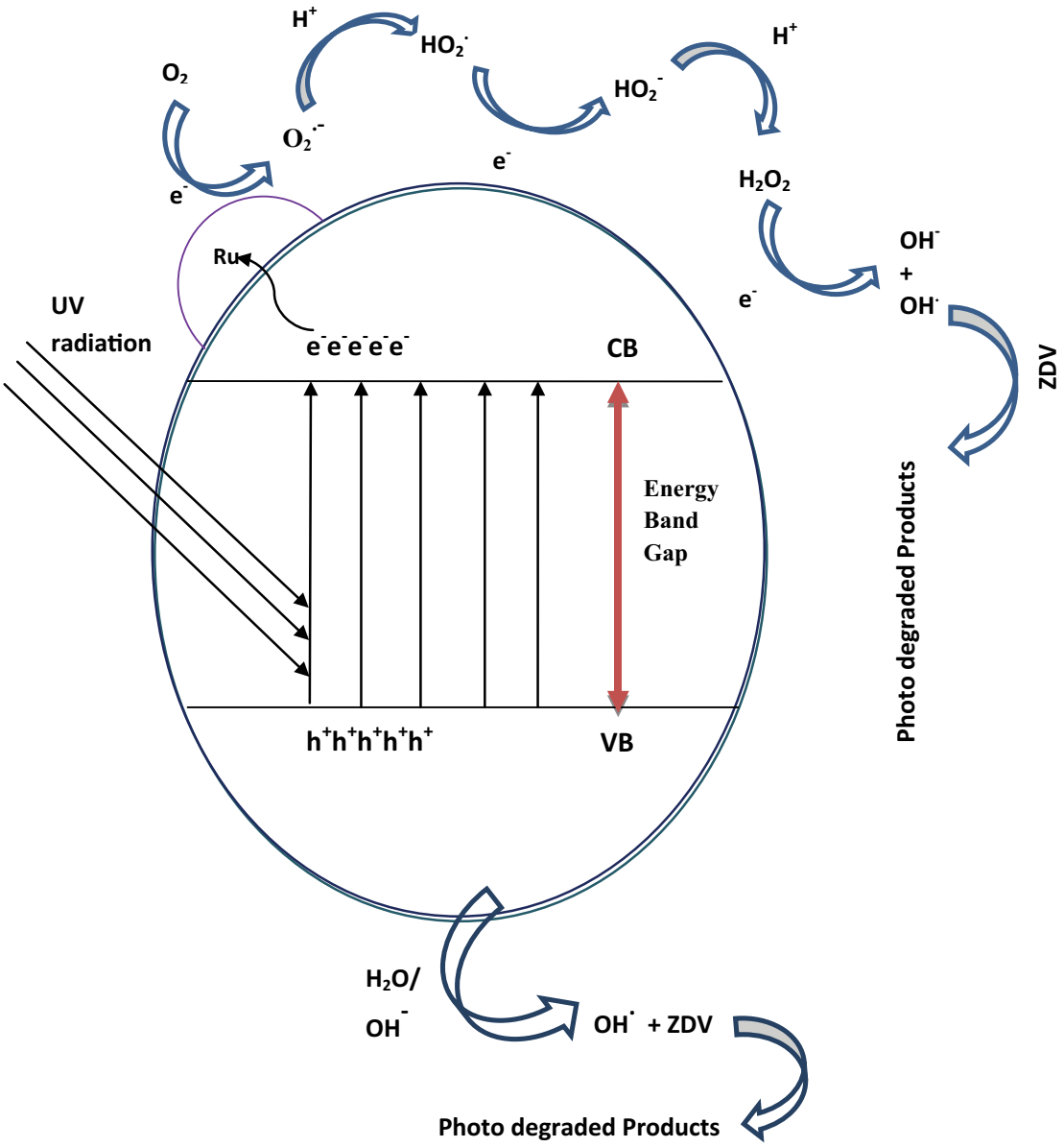

Fig. 11. Photocatalytic electron hole pair mechanism of ZDV with 0.8% (mole ratio) RDTDONPs.

results. Three photo-degraded products of substrate ZDV are analysed and identified by HR-MS. The Liquid impregnation method was used for the preparation of photocatalyst. The higher surface area of 0.8% (mole ratio) RDTDONPs (94.31 m^2/g) enhances its photocatalytic activity and rate of mineralization of substrate ZDV moiety. EDX spectrum of 0.8% (mole ratio) RDTDONPs confirms the presence of only three elements (Ti, O and Ru) and proper doping of ruthenium into the crystal lattice. The experimental data shows that there is a decrease in particle size with an increase in % doping of ruthenium in photocatalyst. The smaller average particle size of 0.8% (mole ratio) RDTDONPs (14.38 nm) obtained from Scherrer equation confirms the increase in the rate of mineralization of substrate ZDV due to the enhancement of photocatalytic activity and surface area. The kinetic measurement confirms that the rate of mineralization of substrate ZDV by 0.8% (mole ratio) RDTDONPs is higher in acidic condition than alkaline condition due to Ru-$TiOH_2^+$ which is found to be a major active species in acidic medium. The kinetic measurement concludes that the rate of mineralization of ZDV enhances with an increase in UV light intensity. The percentage degradation efficiency of substrate ZDV moiety in dark was found to be very low. Experimental results conclude that 0.8% (mole ratio) RDTDONPs enhances the surface charge transfer, increases surface reactivity and decelerates the wasteful recombination of photo-generated electron-hole pair. Experimental results conclude that the percentage degradation efficiency of substrate ZDV is higher with 0.8% (mole ratio) RDTDONPs treatment. Experimental results confirm that the maximum mineralization of substrate ZDV moiety could be attained in 100 min with 0.1 $g\ L^{-1}$ dosage of photocatalyst 0.8% (mole ratio) RDTDONPs,

[ZDV] = 1 × 10^{-5} mol L^{-1}, light intensity = 4 mW cm^{-2} and pH = 4. Experimental results conclude that 0.8% (mole ratio) RDTDONPs is a very efficient photocatalyst for the photo-degradation of ZDV present in environmental waters.

References

[1] O.E. Ligrini, A. Oliveros, A.M. Braun, Photochemical processes for water treatment, Chem. Rev., 93 (1993) 671–698.

[2] V.S. Bhamare, R.M. Kulkarni, Kinetics and mechanistic investigation of Ru(III) catalyzed oxidative degradation of linezolid by permanganate at environmentally relevant pH, Asian J. Chem., 31 (2019) 268–274.

[3] R.M. Kulkarni, V.S. Bhamare, B. Santhakumari, Mechanistic and spectroscopic investigations of Ru^{3+}-catalyzed oxidative degradation of azidothymidine by heptavalent manganese at environmentally relevant pH, Desal. Wat. Treat., 57 (2016) 28349–28362.

[4] J. Hoigne, Inter-calibration of OH radical sources and water quality parameters, Water Sci. Technol., 35 (1997) 1–8.

[5] V.S. Bhamare, R.M. Kulkarni, Photocatalytic degradation of pharmaceutical drug zidovudine by undoped and 5% barium doped zinc oxide nanoparticles during water treatment: synthesis and characterisation, Int. J. App. Pharm., 11 (2019) 227–236.

[6] V.S. Bhamare, R.M. Kulkarni, Synthesis, characterisation and photocatalytic degradation of linezolid during water treatment by ruthenium doped titanium dioxide semiconducting nanoparticles, AIP Conf. Proc., 2142 (2019) 210005.

[7] Md. T. Uddin, Y. Nicolas, C. Olivier, T. Toupance, M.M. Muller, H.J. Kleebe, K. Rachut, J. Ziegler, A. Klein, W. Jaegermann, Preparation of RuO_2/TiO_2 mesoporous heterostructures and rationalization of their enhanced photocatalytic properties by band alignment investigations, J. Phys. Chem. C., 117 (2013) 22098–22110.

[8] Md. T. Uddin, O. Babot, L. Thomas, C. Olivier, M. Redaelli, M. D'Arienzo, F. Morazzoni, W. Jaegermann, N. Rockstroh, H. Junge, T. Toupance, New insights into the photocatalytic properties of RuO_2/TiO_2 mesoporous heterostructures for hydrogen production and organic pollutant photodecomposition, J. Phys. Chem. C., 119 (2015) 7006–7015.

[9] A.A. Ismail, L. Robben, D.W. Bahnemann, Study of the efficiency of UV and visible-light photocatalytic oxidation of methanol on mesoporous RuO_2-TiO_2 nanocomposites, Chemphyschem, 12 (2011) 982–991.

[10] R.M. Kulkarni, R.S. Malladi, M.S. Hanagadakar, M.R. Doddamani, B. Santhakumari, S.D. Kulkarni, Ru-TiO_2 semiconducting nanoparticles for the photo-catalytic degradation of bromothymol blue, J. Mater. Sci. - Mater. Electron., 27 (2016) 13065–13074.

[11] V.S. Bhamare, R.M. Kulkarni, B. Santhakumari, 5% Barium doped zinc oxide semiconductor nanoparticles for the photocatalytic degradation of linezolid: synthesis and characterisation, SN Appl. Sci., 103 (2019) 1–12.

[12] X. Shu, J. He, D. Chen, Visible-light-induced photocatalyst based on nickel titanate nanoparticles, Ind. Eng. Chem. Res., 47 (2008) 4750–4753.

[13] K. Kumar, M. Chitkara, I.S. Sandhu, D. Mehta, S. Kumar, Photocatalytic, optical and magnetic properties of Fe-doped ZnO nanoparticles prepared by chemical route, J. Alloys Compd., 588 (2014) 681–689.

[14] G. Stiver, The treatment of influenza with antiviral drugs, CMAJ, 168 (2003) 49–56.

[15] R.M. Kulkarni, V.S. Bhamare, B. Santhakumari, Oxidative transformation of antiretroviral drug zidovudine during water treatment with permanganate: reaction kinetics and pathways, Desal. Wat. Treat., 57 (2016) 24999–25010.

[16] K. Wetchakun, N. Wetchakun, S. Phanichphant, Enhancement of the Photocatalytic performance of Ru-doped TiO_2 nanoparticles, Adv. Mater. Res., 853 (2008) 55–57.

[17] S. Ozkan, M.W. Kumthekar, G. Karakas, Characterization and temperature-programmed studies over Pd/TiO_2 catalysts for NO reduction with methane, Catal. Today, 40 (1998) 3–14.

[18] A. Taicheng, H. Yang, W. Song, G. Li, H. Luo, J.C. William, Mechanistic considerations for the advanced oxidation treatment of fluroquinolone pharmaceutical compounds using TiO_2 heterogeneous catalysis, J. Phys. Chem. A., 114 (2010) 2569–2575.

[19] M.S. Lee, S.H. Seong, M. Mohseni, Synthesis of photocatalytic nanosized TiO_2-Ag particles with sol-gel method using reduction agent, J. Mol. Catal. A: Chem, 242 (2005) 135–140.

[20] M.B. Muneer, A.A.H. Kadhum, A.B. Mohamad, M.S. Takriff, K. Sopian, Synthesis and catalytic activity of TiO_2 nanoparticles for photochemical oxidation of concentrated chlorophenols under direct solar radiation, Int. J. Electrochem. Sci., 7 (2012) 4871–4888.

[21] M.A. Hema, Y. Arasi, P. Tamilselvi, R. Anbarasan, Titania nanoparticles synthesized by sol-gel technique, Chem. Sci. Trans., 2 (2013) 239–245.

[22] P. Makuła, M. Pacia, W. Macyk, How to correctly determine the band gap energy of modified semiconductor photocatalysts based on UV–Vis spectra, J. Phys. Chem. Lett., 9 (2018) 6814–6817.

[23] A.N. Kadam, R.S. Dhabbe, M.R. Kokate, Y.B. Gaikwad, K.M. Garadkar, Preparation of N doped TiO_2 via microwave-assisted method and its photocatalytic activity for degradation of Malathion, Spectrochim. Acta, Part A, 133 (2014) 669–676.

[24] C.C. Wang, C.K. Lee, M.D. Lyu, L.C. Juang, Photocatalytic degradation of C.I. Basic Violet using TiO_2 catalysts supported by Y. zeolite an investigation of the effects of operational parameters, Dyes Pigm.,76 (2008) 312–319.

[25] J. Sun, L. Qiao, S. Sun, G. Wang, Photocatalytic degradation of Orange G on nitrogen doped TiO_2 catalyst under visible light and sunlight irradiation, J. Hazard. Mater., 155 (2008) 312–319.

[26] S.M. Santhosh, G.R. Balakrishna, Catalysed degradation of indanthrene golden Orange RG in sunlight with vanadium-doped TiO_2, Int. J. Chem. Sci., 6 (2008) 1752–1771.

[27] H. Chun, W. Yizhong, T. Hongxiao, Destruction of phenol aqueous solution by photocatalysis or direct photolysis, Chemosphere, 41 (2000) 1205–1209.

[28] C. Hu, Y. Tang, J.C. Yu, P.K. Wong, Photocatalytic degradation of cationic blue X-GRL adsorbed on TiO_2/SiO_2 photocatalyst, Appl. Catal., B, 40 (2003) 131–140.

[29] U.I. Gaya, A.H.J. Abdullah, Heterogeneous photocatalytic degradation of organic contaminants over titanium dioxide: a review of fundamentals, progress and problems, J. Photochem. Photobiol., C, 9 (2008) 1–12.

[30] I.T. Horvath, Encyclopedia of Catalysis, Wiley, New York, 2003.

[31] N.J. Peill, M.R. Hoffmann, Mathematical model of a photocatalytic fiber-optic cable reactor for heterogeneous photocatalysis, Environ. Sci. Technol., 32 (1998) 398–404.

[32] I.K. Konstantinou, T.A. Albanis, TiO_2-assisted photocatalytic degradation of azo dyes in aqueous solution: kinetic and mechanistic investigations - a review, Appl. Catal., B, 49 (2004) 1–14.

[33] Y. Ohko, T. Tatsuma, A. Fujishima, Characterization of TiO_2 photocatalysis in the gas phase as a photo electrochemical system: behavior of salt-modified system, J. Phys. Chem., 105 (2001) 10016–10021.

[34] N.M. Mahmoodi, M. Arami, N.Y. Limaee, N.S. Tabrizi, Kinetics of heterogeneous photocatalytic degradation of reactive dyes in an immobilized TiO_2 photocatalytic reactor, J. Colloid Interface Sci., 295 (2006) 159–164.

[35] S. Banerjee, J. Gopal, P. Muraleedharan, A.K. Tyagi, B. Raj, Physics and Chemistry of photocatalytic titanium dioxide: visualization of bacterial activity using atomic force microscopy, Curr. Sci., 90 (2006) 1378–1383.

[36] S. Baruah, J. Dutta, Nanotechnology applications in pollution sensing and degradation in agriculture, Environ. Chem. Lett., 7 (2009) 191–204.

[37] C.S. Turchi, D.F. Ollis, Photocatalytic degradation of organic water contaminants: mechanisms involving hydroxyl radical attack, J. Catal., 122 (1990) 178–192.